Available online at www.sciencedirect.com

ScienceDirect

Geochimica et Cosmochimica Acta 265 (2019) 96–108

Geochimica et Cosmochimica Acta

www.elsevier.com/locate/gca

# Biological Fe(II) and As(III) oxidation immobilizes arsenic in micro-oxic environments

Hui Tong [a,b], Chengshuai Liu [b,c,*], Likai Hao [b], Elizabeth D. Swanner [d], Manjia Chen [a], Fangbai Li [a], Yafei Xia [b], Yuhui Liu [b], Yanan Liu [b]

[a] *Guangdong Key Laboratory of Integrated Agro-environmental Pollution Control and Management, Guangdong Institute of Eco-environmental Science & Technology, Guangzhou 510650, China*

[b] *State Key Laboratory of Environmental Geochemistry, Institute of Geochemistry, Chinese Academy of Sciences, Guiyang 550081, China*

[c] *CAS Center for Excellence in Quaternary Science and Global Change, Xi'an 710061, China*

[d] *Department of Geological and Atmospheric Sciences, Iowa State University, Ames 50011, United States*

Received 29 December 2018; accepted in revised form 2 September 2019; available online 10 September 2019

**Abstract**

Fe(III) oxyhydroxides play critical roles in arsenic immobilization due to their strong surface affinity for arsenic. However, the role of bacteria in Fe(II) oxidation and the subsequent immobilization of arsenic has not been thoroughly investigated to date, especially under the micro-oxic conditions present in soils and sediments where these microorganisms thrive. In the present study, we used gel-stabilized gradient systems to investigate arsenic immobilization during microaerophilic microbial Fe (II) oxidation and Fe(III) oxyhydroxide formation. The removal and immobilization of dissolved As(III) and As(V) proceeded via the formation of biogenic Fe(III) oxyhydroxides through microbial Fe(II) oxidation. After 30 days of incubation, the concentration of dissolved arsenic decreased from 600 to 4.8 μg $L^{-1}$. When an Fe(III) oxyhydroxide formed in the presence of As(III), most of the arsenic ultimately was found as As(V), indicating that As(III) oxidation accompanied arsenic immobilization. The structure of the microbial community in As(III) incubations was highly differentiated with respect to the As(V)-bearing ending incubations. The As(III)-containing incubations contained the arsenite oxidase gene, suggesting the potential for microbially mediated As(III) oxidation. The findings of the present study suggest that As(III) immobilization can occur in micro-oxic environments after microbial Fe(II) oxidation and biogenic Fe(III) oxyhydroxide formation via the direct microbial oxidation of As(III) to As(V). This study demonstrates that microbial Fe(II) and As(III) oxidation are important geochemical processes for arsenic immobilization in micro-oxic soils and sediments.


*Keywords:* Iron oxidation; Fe(II)-oxidizing bacteria; Arsenic stabilization; Bioremediation; *aioA* gene

## 1. INTRODUCTION

Arsenic (As) is a naturally occurring metal that can become concentrated in the environment due to irrigation, mining, burning of fossil fuels, and application of pesticides and wood preservatives. These processes have led to the extensive contamination of paddy soils in southern China, leading to elevated levels of arsenic in the rice grown there, which poses a significant risk to public health in populations that use rice as a food staple (Smedley and Kinniburgh, 2002; Muehe and Kappler, 2014; Kumarathilaka et al., 2018). Long-term arsenic exposure causes many adverse health effects, such as nervous system

* Corresponding author at: State Key Laboratory of Environmental Geochemistry, Institute of Geochemistry, Chinese Academy of Sciences, Guiyang 550081, China.

*E-mail address:* liuchengshuai@vip.gyig.ac.cn (C. Liu).

https://doi.org/10.1016/j.gca.2019.09.002
0016-7037/

afflictions, birth defects, diabetes, cancer and skin diseases (Henke, 2009; Meharg and Zhao, 2012). The toxicity and mobility of arsenic is generally a result of its chemical speciation which, in turn, reflects the pH, redox potential, and sorbent species (e.g., metal oxides) in the paddy soils (Smedley and Kinniburgh, 2002). Fe(III) oxyhydroxides are one of the most important sorbent species in iron-rich soils as they have positively charged surfaces at neutral pH and exhibit a strong affinity for arsenic since they form strong inner- and outer-sphere surface complexes (Dixit and Hering, 2003; Sø et al., 2018).

The red paddy soils in southern China have an iron content as high as 2 wt % (Tao et al., 2012). Iron cycling, transformations between oxidized and reduced Fe, and transformation between dissolved and solid species is mainly driven by the microorganisms in the critical zone of the red paddy soils (Weber et al., 2006). Recently, microbial Fe(II) oxidation has been shown to strongly influence the transformation and immobilization of heavy metals due to the formation of biogenic Fe(III) oxyhydroxides (Kumarathilaka et al., 2018). In paddy soils, which have strong oxygen, light, and nitrate gradients when flooded, Fe(II) oxidation can be mediated by three types of Fe(II)-oxidizing bacteria (FeOB), including anoxygenic phototrophic FeOB, microaerophilic FeOB, and anaerobic nitrate-reducing FeOB (Melton et al., 2014). Fe(III) oxyhydroxides formed by phototrophic and nitrate-reducing FeOB under anaerobic conditions have been described in many studies as having the potential to co-precipitate and bind arsenic (Sun et al., 2009; Hohmann et al., 2009; Smith et al., 2017). However, due to the limitations of reproducing the micro-oxic conditions present in paddy soils, the effect of microaerophilic FeOB on arsenic immobilization in these systems remains poorly understood.

Paddy soils are characterized by repeated changes in redox conditions. They become micro-oxic to anoxic during flooding and oxic after draining. Flooding and draining occur during cultivation of a single rice crop. Micro-oxic conditions can occur at the water-soil interface and in the rice rhizosphere of paddy soils where oxygen is evolved in the plant roots (Emerson and Moyer, 1997; Weiss et al., 2004; Chen et al., 2017). These temporal redox shifts and the variation in redox conditions over short spatial scales have important effects on iron cycling and the transformation of heavy metals (Borch et al., 2009). For instance, during flooding, Fe(II) can be produced by microbial Fe(III) reduction, so the Fe(II) concentrations generally increase with depth in soil (Ratering and Schnell, 2001). Then, microaerophilic FeOB can obtain energy for growth through the oxidation of Fe(II) by using oxygen as an electron acceptor in micro-oxic conditions near the soil-water interface or in the rhizosphere. Several groups of exclusively microaerophilic FeOB have been isolated and confirmed to be capable of microaerophilic Fe(II) oxidation, including *Leptothrix*, *Gallionella*, *Sideroxydans*, and *Mariprofundus* (Emerson and Moyer, 1997; Emerson et al., 2007; Fleming et al., 2011; Kato et al., 2013; Chen et al., 2017). These microaerophilic FeOB precipitate biogenic Fe(III) oxyhydroxides at circumneutral pH in the form of twisted ribbon-like stalks, hollow tubular sheaths, and granular or amorphous structures that can adsorb and immobilize organics, arsenic, and other metals (Emerson et al., 2010; Muehe and Kappler, 2014). Although previous studies have shown that biogenic Fe(III) oxyhydroxides formed by FeOB play an important role in arsenic cycling (Hohmann et al., 2009; Xiu et al., 2016; Fernandez-Rojo et al., 2017; Sowers et al., 2017), few studies have explored microaerophilic microbial Fe(II) oxidation for the mechanisms by which arsenic is immobilized by biogenic Fe(III) oxyhydroxides formed from paddy soil microbes under micro-oxic conditions.

Generally, the affinity of As(V) to Fe(III) oxyhydroxides is much stronger than that of As(III). Therefore, the oxidation of As(III) to As(V) decreases the mobility of arsenic. Chemical and microbial oxidation of As(III) to As(V) could increase the immobilization efficiency for arsenic (Mitsunobu et al., 2013). Under micro-oxic conditions at circumneutral pH, the abiotic oxidation of As(III) by oxygen is slow and the oxidation of As(III) is mainly driven by microorganisms (Bissen et al., 2003; Meharg and Zhao, 2012). As(III) oxidation by microorganisms is usually catalyzed by As(III) oxidases, which are encoded by arsenite oxidase genes (*aioA*) (Slyemi and Bonnefoy, 2012). Recent studies have revealed the distribution of the diverse *aioA* in arsenic-contaminated soils and found that some FeOB encoded *aioA* are essential in As(III) oxidation (Fernandez-Rojo et al., 2017; Nitzsche et al., 2015; Zhang et al., 2015). Although arsenic is highly toxic to many microorganisms in paddy soils, some FeOB are able to metabolize arsenic for growth. During the transformation and immobilization of arsenic by Fe(III) oxyhydroxides, arsenic can also affect the distribution and composition of the FeOB via its toxicity. The impact of arsenic on microbial community structure and specifically on the FeOB in micro-oxic paddy soils remains unclear.

Accordingly, the objectives of this study were as follows: (i) to discern the effect of arsenic speciation on the abundance and distribution of microaerophilic FeOB, (ii) to investigate microaerophilic microbial Fe(II) oxidation processes and the products of arsenic immobilization, and (iii) to explore the mechanism of As(III) and As(V) immobilization during microaerophilic microbial Fe(II) oxidation in micro-oxic paddy soils. Soil samples from a paddy field in southern China were used as the inoculum to enrich microaerophilic FeOB using gradient tubes with FeS as the Fe(II) source. The cell growth, Fe(II) oxidation, and chemical speciation of arsenic were determined, and the biogenic minerals were characterized using Mössbauer spectroscopy and X-ray photoelectron spectroscopy (XPS). The changes in the composition and abundance of the microbial community caused by different treatments were profiled over time using 16S rRNA gene-based high-throughput sequencing. Furthermore, the microbial As(III) oxidase genes associated with the different treatments were examined quantitatively in real-time (qPCR) to evaluate the microbial As(III) oxidation. The results of this study are expected to provide a better understanding of arsenic immobilization by biogenic Fe(III) minerals that formed in micro-oxic soils and sediments.

## 2. MATERIALS AND METHODS

### 2.1. Chemicals

As(III) and As(V) stock solutions (20 mM) were prepared by dissolving sodium arsenite ($NaAsO_2$) and disodium hydrogen arsenate heptahydrate salt ($AsHNa_2O_4{\cdot}7H_2O$) (Analytical grade, Sigma Aldrich, USA), which were then sterile-filtered (0.22 μm, Thermo Scientific, USA). All of the other analytical grade chemicals were obtained from the Guangzhou Chemical Co. (Guangzhou, China). The deionized water (18.2 MΩ) was prepared using an ultrapure water system (Easy Pure II RF/UV, Thermo Scientific, USA), and all of the solutions were prepared using deionized water.

### 2.2. Site Description and sampling

The paddy soil samples, which contained orange/brick red-colored flocs (Fe(III) oxyhydroxides), and were collected from Chenzhou, Hunan Province, China (26° 5′15.39″ N, 112°42′38.77″ E) in August 2015 before the rice harvest and under drained soil conditions. Rice was cultivated in the flooded field during the summer, while in the winter the fallow field was drained after harvesting the rice. The physicochemical properties of the paddy soil were as follows: pH (5.86), organic matter (10.2 g $kg^{-1}$), dithionite-citrate-bicarbonate Fe (19.9 g $kg^{-1}$), complex-Fe (5.23 g $kg^{-1}$), and amorphous-Fe (2.32 g $kg^{-1}$). During the sample collection, four equally-sized subsamples were collected from the surface (25 cm length × 25 cm width × 10 ~ 20 cm depth). These subsamples were mixed to form a bulk soil sample. The samples used for cultivation were immediately placed into polyvinylchloride bottles, after which they were stored at 4 °C in a portable cooler. The soil sample used for DNA analysis was frozen and stored in dry ice during transport, and it was stored at −80 °C in the laboratory.

### 2.3. Experimental Setup

Iron(II) sulfide (FeS) was used as an Fe(II) source following the preparation method described by Hanert (2006). Four variations of FeS gradient medium, including liquid, As, semi-solid, and biphasic slant media, were prepared and used as described by Emerson and Moyer (1997). The treatment methods used are presented in Table S1. All of the gradient media contained modified Wolfe's Mineral Medium (MWMM) with an FeS plug. Screw-cap 20 × 125 mm (25 ml) disposable tubes were used for the gradient tube cultures. The bottom layer of 3 ml of FeS colloid contained 1% (w/v) agarose and equal volumes of MWMM and FeS. The top layer of 14 ml of semisolid gradient medium was prepared by adding 0.15% (w/v) agarose to MWMM along with 5 mM of sodium bicarbonate and 1 μl of vitamins solution and trace minerals (Emerson and Moyer, 1997) per milliliter. The pH of the semi-solid gradient medium was adjusted to 6.2 by bubbling with sterile $CO_2$ gas (Emerson and Moyer, 1997). The opposing $O_2$ and Fe(II) gradients that developed in the gel-stabilized semi-solid overlay allowed microaerophilic Fe(II)-oxidizing bacteria to grow at the oxic-anoxic interface (Emerson and Moyer, 1997; Edwards et al., 2003, Fig. S1). To inoculate, equal qualities of soil and sterile water were mixed and 10 μl of suspension was drawn into a pipette tip and inserted above the FeS layer. For As-immobilization experiments, 16 μM As(III) and As(V) from sterile 20 mM $NaAsO_2$ and $AsHNa_2O_4$ stock solutions, respectively, were added to the semi-solid gradient medium. The enrichments were cultured in the dark at 25 ± 1 °C.

### 2.4. Analytical methods

**Iron and arsenic determination.** Total iron concentration of the iron oxide layer (the cell growth band with Fe(III) oxyhydroxides) was defined as the iron oxide layer in Fig. S1) was determined using the 1,10-phenanthroline colorimetric method after hydroxylamine reduction (Fredrickson and Gorby, 1996). To calculate the rate of Fe(II) oxidation, the accumulated total iron at the oxic-anoxic interface was measured at discrete time points. At each point in time, the entire iron oxide layer in each inoculated treatment was collected and centrifuged, followed by removal of the supernatant. The pellet (Fe(III) oxyhydroxides) was then mixed with MilliQ water to reach a total volume of 2 ml. Then the same volume of mixture for each time point was diluted into a known amount of a solution of 0.5 M HCl for 1.5 h of incubation. For the control treatments, the samples were removed for total iron determination at the same depths as inoculated treatments. The position of iron oxide layer varied slightly from tube to tube. Therefore, the sampling depths for control treatments were taken at the same depth as the inoculated treatments, which was determined at each time point. The dissolved 0.5 M HCl solution was reduced using hydroxylamine and analyzed using a spectrophotometer (Shimadzu, Kyoto, Japan) at 510 nm. In the inoculated experiments, the entire iron oxide layer was collected and filtered to determine the arsenic concentration (total arsenic, As(III), and As(V)). In the killed control and no-FeS experiments, the semi-solid medium from the same depth in the gradient tubes was collected to determine the arsenic concentration. To analyze the dissolved As, the suspension from the Fe(II) oxidation zone was sterile filtered (0.22 μm) in an anaerobic chamber, and then acidified using 10 μl of 65% $HNO_3$ to preserve the As speciation (Sun et al., 2009). The arsenic species in the solid (Fe(III) oxyhydroxides) were dissolved in 6 M HCl. Total As was quantified on an inductively coupled plasma mass spectrometry (ICP-MS, NexION 300X, Perkin-Elmer) (Sun et al., 2009). The As(III) and As(V) concentrations were determined on an ICP-MS equipped with a high performance liquid chromatography column (HPLC) to separate the As(III) and As(V) (Mitsunobu et al., 2013). To differentiate between arsenic adsorption to surfaces and co-precipitation into Fe(III) oxyhydroxides, an extraction protocol involving NaOH was used to desorb the arsenic from the Fe(III) oxyhydroxides (Huhmann et al., 2017). After 30 days of incubation, the entire iron oxide layer of each inoculated treatment was collected and centrifuged to remove the supernatant. The solids were

mixed with 1 M NaOH for 4 h in the dark on a rotator. After the reaction, the suspensions were centrifuged and the supernatant was collected. The extracted solution, representing adsorbed arsenic, was filtered and analyzed with ICP-MS to quantify the extracted arsenic. The remaining solids were dissolved in 6 M HCl to quantify the co-precipitated arsenic.

The detailed procedures used for the X-ray photoelectron spectroscopy (XPS), Mössbauer spectroscopy, cell numeration, and electron microscopy are provided in Appendix A (Text S1).

### 2.5. DNA extraction, quantitative real-time PCR (qPCR), high-throughput sequencing, and bioinformatics analysis

DNA was extracted from the iron oxide layer of the enrichment using a PowerSoil™ DNA isolation kit (MO BIO Laboratories, Inc., USA). A sterile pipette was used to remove as much of the agarose overlying the growth band as possible. The gel, including the growth band, was heated at 70 °C in a water bath for 12 min to melt the agarose. Then, it was centrifuged at 10,000*g* for 5 min (Emerson and Moyer, 1997). The supernatant was discarded, and the pellets composed of iron oxides and cells were re-suspended in 300 µl of deinoized water for DNA extraction. Polymerase chain reaction (PCR) amplification of the 16S rRNA gene fragments (V4 region) was performed using Illumina-specific fusion primers, i.e., F515 (5′-GTGCCAG CMGCCGCGGTAA-3′) and R806 (5′-GGACTACVSGG GTATCTAAT-3′), with a sample-specific 12-bp barcode added to the reverse primer for both the total genomic DNA extract and the DNA fraction (Liu et al., 2007). Then, unique barcodes were added to the sample in each well to enable pooling. The 16S rRNA gene amplicons were submitted to Magigen Biotechnology (Guangzhou, China) for Miseq Illumina high-throughput sequencing. The bioinformatics analysis method is described in Appendix A (Text S2). The genomic datasets were deposited in the NCBI under BioProject ID PRJNA381404 and accession number SRP5408992.

The abundances of the *aioA* gene in the gradient tube bands, encoding the large catalytic subunit of the As(III) oxidase, were determined using the qPCR with a MyiQ™2 Optics Module (BIO-RAD, USA) with primers aoxBM4-1F and aoxBM2-1R (Fernandez-Rojo et al., 2017). Total bacterial abundance was measured using the qPCR of the 16S rRNA gene and universal bacterial primers 519F and 1406R (Tong et al., 2014). The qPCR calibration curves were generated from serial dilutions of plasmids containing the cloned target sequences. The corresponding gene copy number was calculated relative to the plasmid sizes, insert lengths and Avogadro numbers (Whelan et al., 2003).

## 3. RESULTS

### 3.1. Fe(III) Oxyhydroxides formed by microaerophilic Fe (II)-oxidizing bacteria

Microbial enrichment was accomplished by inoculating the Fe gradient tubes with the Fe floculant-containing soils (Fig. S1). After 3–5 days of incubation, a zone of cell growth was observed 1–2 cm below the medium surface, visible as a thin orange band of iron oxides. Concomitantly, the amount of Fe precipitate increased and an iron oxide layer gradually formed in the gradient tube with increasing incubation time. A plot of total Fe versus cell growth is presented in Fig. 1. For all of the treatments with inocula, the amount of Fe precipitate increased for the first 20 days, and then, it remained stable. The rate of iron oxidation, which was indicated by the total iron accumulation, in the treatment with the original soil was higher than those of the FeS gradient tubes without inocula and tubes with arsenic during incubation (Fig. 1A). The addition of arsenic affected the rate of Fe(II) oxidation. The rate of total Fe precipitation calculated using the pseudo first-order exponential decay model was either $0.137 \pm 0.045$ or $0.119 \pm 0.030$ mM $d^{-1}$, depending on the As(III) or As(V) levels introduced into the treatments. A higher rate of Fe precipitation ($0.197 \pm 0.034$ mM $d^{-1}$) was observed for the treatment without arsenic. The Fe precipitation trends were are consistent with the potential microaerophilic FeOB growth, with higher FeOB growth yields in the absence of arsenic than in the presence of As(III) (Fig. 1B).

The SEM images reveal that most of the cells were encrusted with nano-sized amorphous iron minerals regardless of whether arsenic was present or not (Fig. S2). The bacteria are rods approximately $1.0 \sim 3.0$ µm in diameter. The cell surfaces were partly or entirely encrusted with mineral precipitates. The precipitates were formed by microaerophilic bacteria at circumneutral pH under micro-oxic conditions. Mössbauer spectroscopy results obtained at 12 K for the precipitates are shown in Fig. 2, and the corresponding fit parameters are presented in Table S2. The negative quadrupole splitting (QS) and center shift (CS) Fe(III) oxides values are similar to those reported by Chen et al. (2019), which were identified as ferrihydrite. The Mössbauer data clearly shows that the main Fe(III) oxide phase (>95% of total Fe) in all of the inoculated treatments was ferrihydrite.

### 3.2. Arsenic immobilization by Fe(III) oxyhydroxides formed by microaerophilic Fe(II)-oxidizing bacteria

The trends in total soluble As during microaerophilic microbial Fe(II) oxidation are shown in Fig. 3. During microbial Fe(II) oxidation, the As(III) and As(V) in the solution were effectively sorbed/immobilized by the newly formed Fe(III) oxyhydroxides. In all treatments with inocula, more than 98% of the added As(III) and As(V) was adsorbed/immobilized. Overall, the As(III) and As(V) sorption/immobilization rates observed in the biogenic treatments were 0.104 and 0.148 µg $L^{-1}$ $d^{-1}$, respectively. In the abiotic control, the As removal was attributed to the chemical oxidation of Fe(II) by limited oxygen diffusion. In this case, the sorption/immobilization of As(V) was stronger than that of As(III) in all treatments. In the As (III) treatments with inocula, the arsenic extracted from precipitates contained some As(V), indicating that some As(III) was oxidized (Fig. S3). No As(III) was observed in As(V) treatments (data not shown). The X-ray

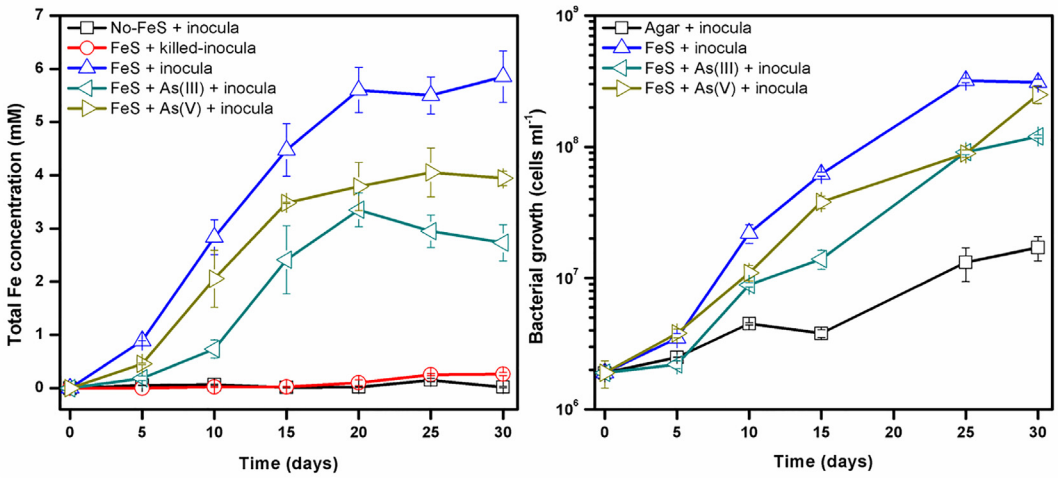


Fig. 1. Time-dependent changes in total Fe concentrations of the cell bands (A) and cell growth (B) in the treatments of inocula, killed-inocula with FeS, and agarose only control. For all treatments (including the inocula and control treatments), the samples for total Fe were collected at the same height of gradient tubes. Error bars show the standard errors from three replicates.

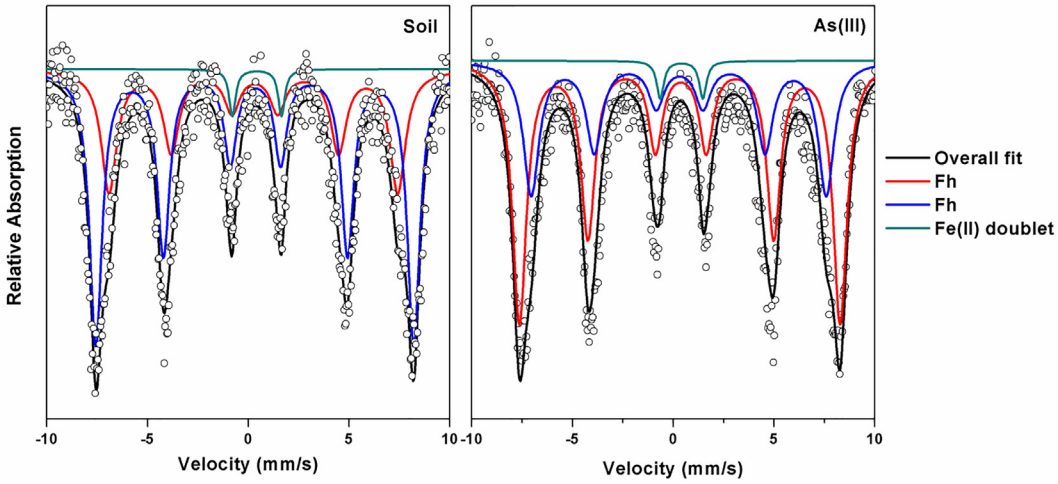


Fig. 2. Fitted Mössbauer spectra of the precipitation formed by microaerophilic microorganisms in the presence or absence of As(III) at 12 K. Corresponding fit parameters are summarized in Table S2.

photoelectron spectroscopy (XPS) results of samples from arsenic treatments were compared with the spectrum of $As_2O_3$ and $As_2O_5$ standards, revealing the presence of As (V) in the treatments incubated with As(III) (Fig. S4).

Immobilized arsenic can be adsorbed onto or co-precipitated with Fe(III) oxyhydroxides. Wet chemical extraction with NaOH solution was used to distinguish between the adsorbed arsenic and the co-precipitated arsenic. After incubation for 30 days, NaOH extraction and complete the dissolution of the Fe(III) oxyhydroxides, $28 \pm 4\%$ of the adsorbed arsenic and $69 \pm 8\%$ of the co-precipitated arsenic were recovered from the As(III) treatment, while $22 \pm 5\%$ of the adsorbed arsenic and $79 \pm 6\%$ of the co-precipitated arsenic were recovered from the As (V) treatment (Fig. S5). These results indicate that arsenic preferentially co-precipitates with the Fe(III) oxyhydroxides during microaerophilic microbial Fe(II) oxidation under micro-oxic conditions.

### 3.3. Microaerophilic bacteria community composition during microbial Fe(II) oxidation

A total of 1,089,166 quality sequences for all treatments (incubation without arsenic, and incubation with As(III) and/or As(V)) were generated via Illumina high-throughput sequencing. The sequence frequencies of the individual samples ranged from 42,536 to 79,136 (Table S3). Viewed with different alpha-diversity indexes (Simpson and Shannon), the microbial diversities were found to be higher in the absence of arsenic than in the presence of arsenic (Table S3).

As for the composition of the microbial community in the original soil, a comparisons of the incubation treatments with As(III) or As(V) and the incubation treatments without arsenic were conducted using principal coordinate analysis (PCoA). The results show that the structures of the microbial communities in the treatments with As(III)

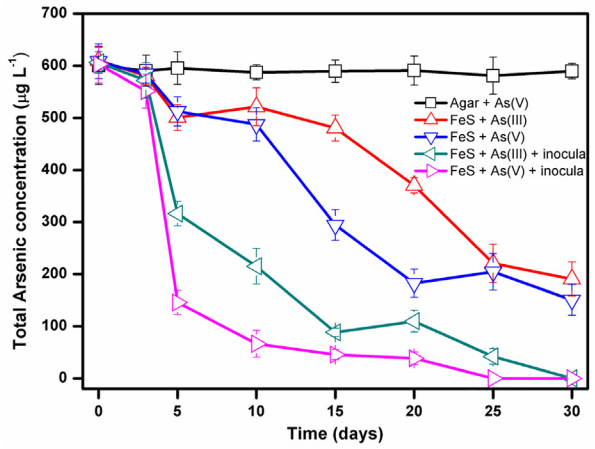


Fig. 3. Time-dependent changes in total arsenic [As(III) + As(V)] concentrations in the dissolved phase from gradient tube bands in the treatments of inocula and non-inocula with arsenic and FeS, and agarose with arsenic control. For all treatments (including the inocula and control treatments), the samples for total arsenic were collected at the same depth of gradient tubes. Error bars show the standard errors from three replicates.

or As(V) differed greatly from those of the original soil and the treatment without arsenic (Fig. 4). In addition, a clear shift in the microbial communities of the two treatments with As(III) and As(V) was observed, which also indicates

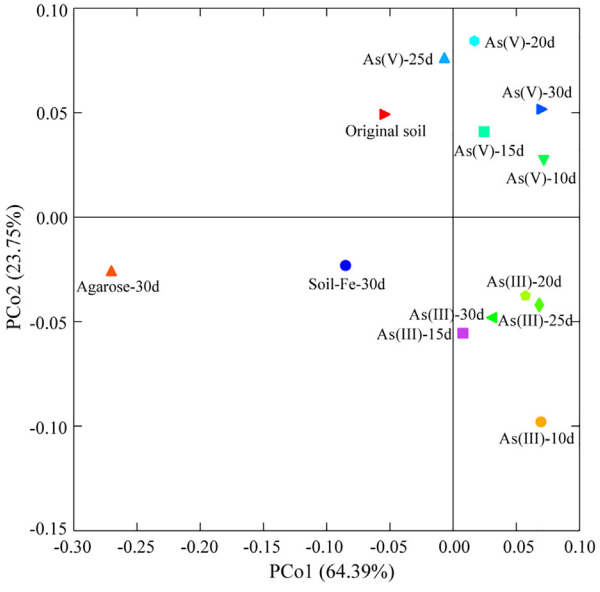


Fig. 4. PCoA compares microbial composition to As(III) and As (V)-amended incubation. Original soil denotes the inoculum source prior to microcosms; agarose-30d denotes the sample with only agarose after 30 days; soil-Fe(II)-30d denotes the sample with Fe (II) after 30 days; As(III)-10d, As(III)-15d, As(III)-20d, As(III)-25d, and As(III)-30d denote the sample with As(III) after 10, 15, 20, 25, and 30 days, respectively; As(V)-10d, As(V)-15d, As(V)-20d, As(V)-25d, and As(V)-30d denote the sample with As(V) after 5, 10, 15, 20, 25, and 30 days, respectively.

that arsenic speciation significantly affected the microbial community during Fe(II) oxidation.

The most abundant genera of all treatments are shown in Fig. 5. The dominant classes of *Proteobacteria* in the original soil include *Alphaproteobacteria* and *Betaproteobacteria*, including the genera *Curvibacter*, *Cupriavidus*, *Duganella*, *Polaromonas*, *Afipia*, *Ramlibacter*, and *Dongia*. Taxa belonging to the *Sphingobacteria* class of *Sediminibacterium* were also found in the original soil. After 30 days of incubation with Fe(II), the dominant genera were *Curvibacter*, *Pseudomonas*, *Cupriavidus*, *Sediminibacterium*, *Duganella*, *Polaromonas*, *Ralstonia*, and *Sphingomonas*, while without Fe(II) (only agarose), the dominant genera were *Bdellovibrio*, *Cupriavidus*, *Stakelama*, *Sphingomonas*, *Phenylobactera*, Pseudogulbenk, and *Caulobacter*. After 30 days of treatment with As(III), the dominant genera were *Curvibacter*, *Pseudomonas*, *Cupriavidus,* *Duganella*, *Polaromonas*, and *Ralstonia*, while for the As(V) treatment, they were *Curvibacter*, *Pseudomonas*, *Cupriavidus*, *Sediminibacterium*, *Pseudomonas*, and *Stakelama*.

To evaluate the potential contributions of microbially mediated As(III) oxidation to arsenic immobilization, the copy numbers of *aioA* genes were determined via qPCR (Fig. 6). The results show that *aioA* genes appeared soon after incubation and that the number of copies of *aioA* genes in the As(III) treatments was higher than that in the As(V) treatments.

## 4. DISCUSSION

### 4.1. Fe(II) oxidation with microaerophilic Fe(II)-oxidizing bacteria

Culturing is currently the most direct method of proving microbial involvement in Fe(II) oxidation due to the lack of mineralogical biosignatures for FeOB (Chan et al., 2016). Therefore, the development of Fe(II)/$O_2$ gradients was used to enrich and isolate the microaerophilic FeOB, many of which are likely to be autotrophic for supporting a community of other microorganisms (Weiss et al., 2007; Picardal et al., 2011). Differences in the composition of the microbial communities of the original soil treatment and the treatment with only agarose suggest that semi-solid gradient tubes can effectively be used to enrich microaerophilic microorganisms. The dominant genera enriched in the treatments with Fe(II) (Fig. 5) contained more genera that have documented ad FeOB in previous studies (Emerson et al., 2010; Swanner et al., 2011; Shelobolina et al., 2012; Xiu et al., 2016; Hassan et al., 2016) than the agarose only incubations, confirming the effectiveness of the gradient tube in enriching potential microaerophilic FeOB. Many of these microaerophilic FeOB can produce extracellular organic fibers, forming twisted stalks or sheaths and acting as a precipitation template for iron oxides in order to avoid encrustation (Schädler et al., 2009), while others do not produce such structures (Swanner et al., 2011). However, in present study, the cells were encrusted by mineral precipitation (Fig. S2). The encrustation of microaerophilic FeOB during Fe(II) oxidation has previously been reported. This has been ascribed to: (i) microaerophilic FeOB-formed

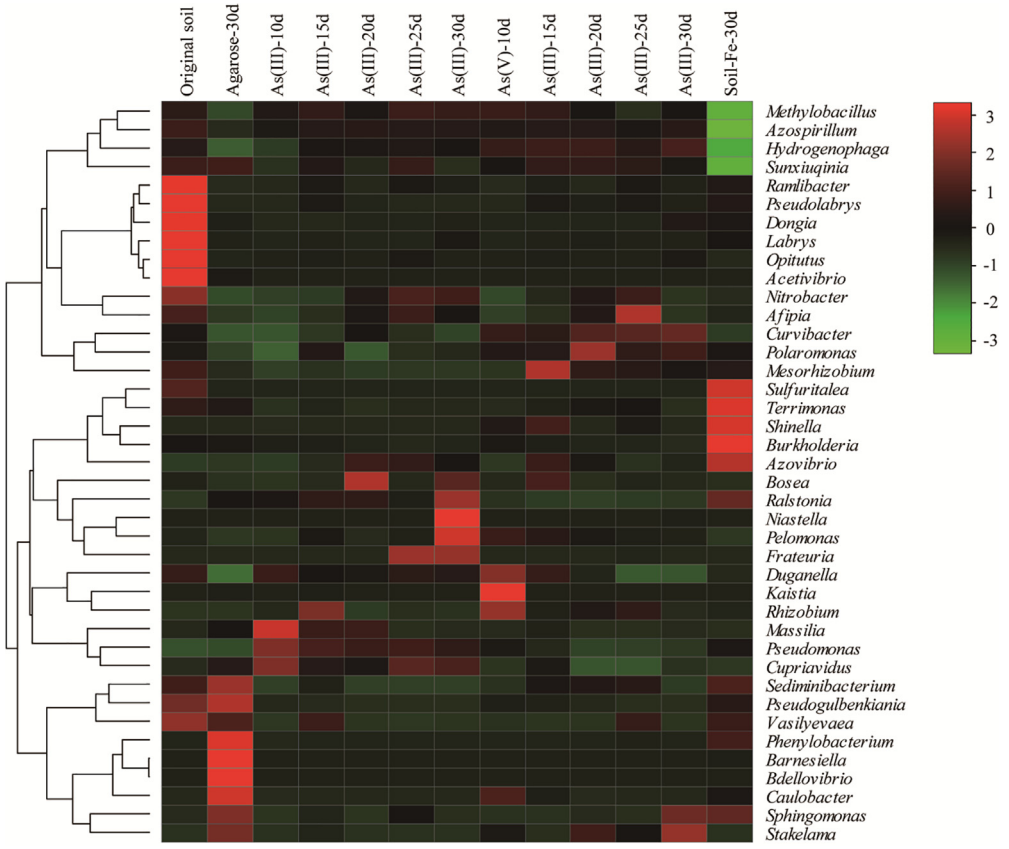


Fig. 5. Relative abundance of top 40 genera in the cell band of different treatments revealed by 16S rRNA high-throughput sequencing. Original soil denotes the inoculum source prior to microcosms; agarose-30d denotes the sample with only agarose after 30 days; soil-Fe(II)-30d denotes the sample with Fe(II) after 30 days; As(III)-10d, As(III)-15d, As(III)-20d, As(III)-25d, and As(III)-30d denote the sample with As(III) after 10, 15, 20, 25, and 30 days, respectively; As(V)-10d, As(V)-15d, As(V)-20d, As(V)-25d, and As(V)-30d denote the sample with As (V) after 5, 10, 15, 20, 25, and 30 days, respectively.

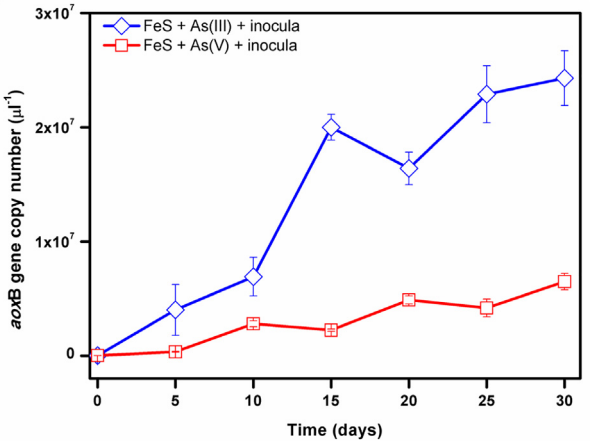


Fig. 6. Copy numbers of *aioA* genes in Fe(II) biogenic precipitation with As(III) and As(V).

stalks or sheaths, which were covered by mineral precipitation near or on cells (Lin et al., 2012; Fleming et al., 2014), and (ii) stalks or sheaths formed by microaerophilic FeOB, which were not preserved because they easily disaggregated (Chan et al., 2016). In the present study, however, there was no direct evidence to confirm which microaerophilic microorganisms were oxidizing F(II), or to determine how microaerophilic FeOB encrusted during Fe(II) oxidation under micro-oxic conditions. In the future, a dilution series could be used to isolate microaerophilic FeOB from this filed site to elucidate the mechanism of microbial Fe(II) oxidation and cell encrustation.

Under micro-oxic conditions ($O_2 < 50$ μM), microaerophilic FeOB can successfully compete with abiotic Fe(II) oxidation by $O_2$ at circumneutral pH (Chan et al, 2016). Fe(II) is subject to microbial oxidation by microaerphilic FeOB to produce Fe(III), which results in hydrolyzation and precipitation as Fe(III) oxyhydroxide in the gradient tubes (Fig. S1). The Fe(III) precipitation was identified as ferrihydrite by Mössbauer spectroscopy. As reported previously, the biogenic Fe(III) precipitation produced by the microaerophilic FeOB is always a poorly crystalline form of ferrihydrite (Emerson et al., 2010). However, the oxygen concentration, the composition of medium, and the availability of electron shuttles can influence the iron oxidation rate, which affected the forms of the mineral products. For example, lepidocrocite was the primary Fe(III) oxyhydroxide in the oxygen deficient zones (Heller et al., 2017), while

hydrous ferric oxide, 2-line ferrihydrite, and lepidocrocite were the primary Fe(III) oxyhydroxide formed in the presence of phosphate, silicate, and calcium in the different Fe (III) precipitation gradients formed at redox transitions (Voegelin et al., 2010; Senn et al., 2015). In addition, the presence of adsorbed arsenic affects minerals growth (Hohmann et al., 2009), which can lead to a decreasing iron mineral particle size, thus increasing the surface area (Fuller et al., 1993). This might facilitate arsenic adsorption and/or co-precipitation. During Fe(II) oxidation, arsenic can also be co-precipitated with Fe(III), resulting in the formation of amorphous ferric arsenate (Fernandez-Rojo et al., 2017; Tian et al., 2017). In this study, although a large proportion of arsenic was co-precipitated during Fe(III) precipitation (Fig. S5), Mössbauer spectroscopy did not detect the presence of amorphous ferric arsenate in the precipitates (Wu et al., 2018).

The presence of arsenic decreased the rate of Fe(II) oxidation and the growth of microaerophilic bacteria (Fig. 1), which was ascribed to the possible toxicity of arsenic in microbial metabolism. In addition, the rate of iron oxidation in the presence of As(V) was higher than that in the presence of As(III). This suggests that As(III) has a stronger inhibitory effect on microbial Fe(II) oxidation than As (V) does, likely due to the higher toxicity of As(III) (Hohmann et al., 2009). Similar results were observed for other FeOB in the presence of arsenic, such as *Pseudomonas* sp. strain GE-1, *Pseudogulbenkiania* sp. strain 2002, *Acidovorax* sp., and *Rhodobacter ferrooxidans* strain SW2 and strain KS (Hohmann et al., 2009; Xiu et al., 2015, 2016).

### 4.2. Arsenic immobilization during microaerophilic microbial Fe(II) oxidation

In this study, ferrihydrite was found to be the predominant Fe(III) precipitate in both the absence and presence of arsenic. Generally, the ferrihydrite formed by FeOB has a large surface area, which facilitates the adsorption of arsenic (Fuller et al., 1993; Sowers et al., 2017). A previous study concluded that the incorporation of arsenic into Fe (III) oxyhydroxides can produce amorphous ferric arsenate (or amorphous scorodite), which further accelerated arsenic immobilization (Tian et al., 2017). Therefore, ferrihydrite formation and arsenic incorporation can promote arsenic immobilization in micro-oxic conditions. During arsenic immobilization, arsenic co-precipitation may be as important to the formation of Fe(III) oxyhydroxides as adsorption (Hohmann et al., 2009). In the present study, wet chemical extraction with NaOH was used to distinguish between adsorbed arsenic and co-precipitated arsenic, and the results indicated that co-precipitation led to a more efficient arsenic removal than adsorption (Fig. S5), which is consistent with the results of previous reports (Xiu et al., 2015; Huhmann et al., 2017). In the As(V) treatments, the proportion of precipitated arsenic was larger than that in the As(III) treatments, indicating that As(V) was preferentially partitioned into the solid phase (Mitsunobu et al., 2013). This may be due to the maximization of the number of coordination sites, such as occurs in neutralization of acidic As(V)-Fe(III) solutions, which provides more surface sites for reaction between As(V) and Fe(III) (Jia and Demopoulos, 2005).

As(V) was detected in the As(III) treatment, but no As (III) was detected in the As(V) treatment, indicating that As(III) oxidation, but not As(V) reduction, occurred during microaerophilic microbial Fe(II) oxidation. As(III) oxidation in natural environments is usually caused by both biotic and abiotic reactions. In the control treatment without inocula or killed-inocula (also forming Fe(III) oxyhydroxides), less than 5% of the As(III) was oxidized, while over 80% of the As(III) was oxidized in the inoculated treatments after 30 days (data not shown). This indicates that abiotic As(III) oxidation was minor, and supported the role of bacterial As(III) oxidation during microaerobic Fe(II) oxidation (Mitsunobu et al., 2013). A previous report concluded that during microbial Fe(II) oxidation, colloidal Fe (II) and Fe(III) species can be formed as Fe(III) is precipitated (Swanner et al., 2011, 2015). These colloidal intermediates could increase the As(III) adsorption and produce As (III)-Fe(II/III) complexation, which would also change the iron and arsenic redox potentials and reactivities (Ding et al., 2018). The direct contact of bacteria with complexed and/or colloidal Fe(II)-Fe(III) and As(III) could result in the more efficient oxidation of As(III) in the inoculated experiments (Fig. S4). The oxidation of the more toxic species of As(III) to the less toxic species of As(V) is a detoxification strategy used by some special bacteria to reduce the harmful effect of arsenic on the microaerophilic FeOB (Hohmann et al., 2009). Additionally, with the higher affinity of As(V) for Fe(III) oxyhydroxides than that of As(III), the oxidation of As(III) to As(V) can decrease the mobility of arsenic by producing Fe(III) oxyhydroxides (Mitsunobu et al., 2013; Zhang et al., 2017).

Two reactions were responsible for arsenic immobilization during microaerophilic Fe(II) oxidative mineralization. First, FeOB oxidized Fe(II) into Fe(III) to form Fe(III) oxyhydroxides at the oxic-anoxic interfaces. Then, As(III) or As(V) was adsorbed and/or co-precipitated by electrostatic interactions and/or direct covalent bonds with Fe (III) oxyhydroxides (Xiu et al., 2016; Sowers et al., 2017). Finally, the As(III), which was directly sequestered by Fe (III) oxyhydroxides, was oxidized into As(V), while As(V) immobilization occurred through direct adsorption and/or co-precipitation. Based on the above discussion, the proposed mechanisms for the immobilization of As(III) and As(V) by microaerophilic microorganisms are schematically illustrated in Fig. 7.

### 4.3. Dominant microorganisms for microaerophilic Fe(II) oxidation coupled with arsenic immobilization

Micro-oxic environments allow for Fe(II) oxidation and formation of Fe(III) oxyhydroxides, providing binding sites for arsenic immobilization. In the present study, biogenic Fe(III) oxyhydroxides produced after microaerophilic Fe (II) oxidation were shown to adsorb and co-precipitate both As(III) and As(V) (Figs. 3 and S5). These results highlight the important role of microaerophilic microorganisms in Fe(II) oxidative mineralization and the immobilization

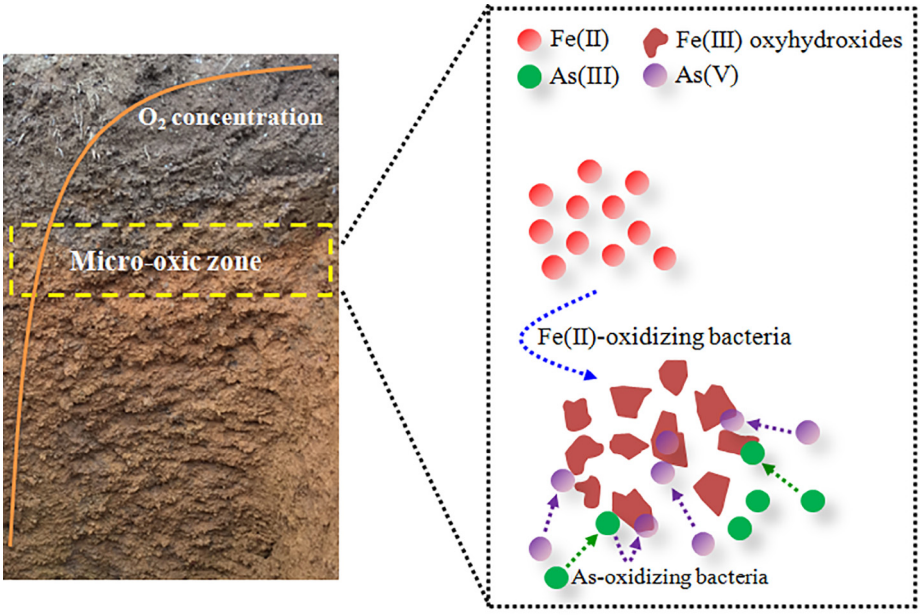


Fig. 7. Schematic illustration of As(III) and As(V) removal by Fe(II) biogenic precipitation.

of arsenic in micro-oxic environments. The abundances of the dominant microaerophilic microorganisms during Fe (II) oxidation are shown in Fig. S6. *Curvibacter*, *Cupriavidus*, and *Sediminibacterium* were abundant in all treatments. However, other dominant genera were more abundant in the presence of Fe(II) than the treatments with only agarose. *Curvibacter*, *Cupriavidus*, *Duganella*, *Polaromonas*, *Pseudomonas*, *Ralstonia*, and *Sediminibacterium* were enriched in the gradient tubes, all of which have been identified as FeOB in previous reports (Swanner et al., 2011; Shelobolina et al., 2012; Hassan et al., 2016; Xiu et al., 2016). These results suggest that FeOB can outcompete other microaerophilic microorganisms under selective culturing conditions, e.g., in gradient tubes with Fe(II) as an electron donor.

In paddy soils or aquifers with opposing redox gradients, Fe(II) oxidation has been observed at high arsenic concentrations, and the mobile arsenic is quickly absorbed and co-precipitated with the Fe(III) oxyhydroxides formed through microbial Fe(II) oxidation, as observed in other studies (Smedley and Kinniburgh, 2002; Meharg and Rahman, 2003). This indicates that the microorganisms involved in the microaerophilic Fe(II) oxidation in the present study can effectively immobilize arsenic. In the present study, several microaerophilic microorganisms were enriched in the iron oxide layer, including *Curvibacter*, *Cupriavidus*, *Ralstonia*, *Sediminibacterium* and *Pseudomonas*, which are genera known to oxidize Fe(II) (Swanner et al., 2011; Shelobolina et al., 2012; Hassan et al., 2016; Xiu et al., 2016). The results confirmed efficient arsenic immobilization following microaerophilic microbial Fe(II) oxidation. Previous studies have suggested that the Fe(III) oxyhydroxides formed by the FeOB are a sink for metals (Liu et al., 2008). However, our SEM results show that the microaerophilic microorganisms were covered with Fe(III) oxyhydroxides (Fig. S2), but still grew well (Fig. 1), indicating that some microorganisms may have the ability to resist high metal concentrations and to utilize these metals for growth. In the present study, *Cupriavidus*, *Ralstonia*, and *Pseudomonas* were the most abundant species in the arsenic treatments, indicating that these microorganisms likely had a high metal tolerance and/or participated during arsenic immobilization (Canovas et al., 2003; Rozycki and Nies, 2009).

Previous reports show that arsenic is toxic to many microorganisms, which consequently affects the distribution of FeOB (Fernandez-Rojo et al., 2017). The cluster analysis showed that the structure of microbial community in the iron oxide layer was significantly affected by the presence of arsenic (Fig. S7). Variations in the structure and activity of the microbial community may affect the Fe(II) oxidation rate. Additionally, the structures of the microbial community in the As(III) and As(V) treatments were found to differ considerably. After 30 days of incubation, the results showed that the relative abundances of the *Curvibacter* and *Sediminibacterium* FeOB in the As(III) treatments were lower than those observed in the treatments with As(V) and without arsenic. These results indicate that As(III) is more toxic to FeOB than As(V). Although As(III) is harmful to many microorganisms, some microorganisms are expected to tolerate arsenic and to overcome its toxicity (Hohmann et al., 2009). For example, the relative abundances of *Pseudomonas* and *Ralstonia* were found to be higher than those of other species in the As(III) treatments. The ICP and XPS results show that As(V) accumulated in the Fe(III) oxyhydroxides in the As(III) treatments (Figs. S3 and S4), suggesting that As(III) oxidation also occurred in the iron oxide layer. Additionally, the identification results for *aioA* genes indicate that microbially mediated As(III) oxidation occurred in the As(III) treatments, which is consistent with

the results of previous reports (Casiot et al., 2003; Mitsunobu et al., 2013; Fernandez-Rojo et al., 2017).

Microbial As(III) oxidation can be catalyzed by As(III) oxidase during both aerobic and anaerobic As(III) oxidation (Jia et al., 2014). In the present study, the relative abundances of *aioA*-carrying bacteria in the Fe(III) oxyhydroxides with As(III) were higher than those without As (III) (Fig. 6), indicating that arsenic can stimulate *aioA* gene expression and can sustain arsenic-oxidizing activity (Casiot et al., 2003). The *aioA* genes have been reported to be the most abundant among the *aioA*, arsenate respiring gene (*arrA*), arsenate reductase (*arsC*), and adenosylmethionine methyltransferase (*arsM*) in 13 paddy soils collected from southern China (Zhang et al., 2015). In addition, As(V) was the dominant arsenic species in these soils, indicating a high potential for microbial arsenic oxidation by the *aioA* gene in arsenic contaminated soils. Therefore, we concluded that the greater the abundance of *aioA* gene in paddy soil, the more extensive the oxidation of As(III) to As(V). In addition, the ratios of the *aioA* gene copies relative to the universal bacterial 16S rRNA gene copies (*aioA*/16S rRNA) were estimates of the proportion of As(III)-oxidizers harboring *aioA* gene in the bacterial communities in the As(III) treatments. In the present study, the ratios ranged from 0.88% to 5.97% for the different time points (Fig. S8), which is similar to the results of previous reports of As-polluted acid mine drainage and rivers (Quéméneur et al., 2010; Fernandez-Rojo et al., 2017). These high ratios suggest that the As(III)-oxidizing bacteria are potential contributors to As(III) oxidation, leading to an increase in the As(V) fraction in Fe(III) precipitation (Fig. S3). In the present study, the gradient tubes with FeS were mainly used to enrich the potential microaerophilic FeOB. Enriched bacteria, such as *Pseudomonas*, *Cupriavidus*, *Polaromonas*, and *Ralstonia*, can oxidize As(III) as well as Fe(II) (Xiu et al., 2016; Zhang et al., 2015).

Homologs of genes encoding respiratory arsenite oxidase (*aioA*) have been found in *Cupriavidus* and *Ralstonia* (Lieutaud et al., 2010), which were enriched in the arsenic treatments. The numbers of copies of the *aioA* gene increased at the start of the incubation, and then reached a stable stage, which echoes the changes in the As(III) concentrations. In addition to the function of As(III) oxidation, some of the Fe(II)-oxidizing bacteria, such as *Cupriavidus*, *Sediminibacterium,* and *Ralstonia*, can influence both Fe(II) oxidation and As(III) oxidation in micro-oxic conditions. However, compared with the As (III) treatments, higher rates of Fe(II) oxidation and Fe precipitation were observed in the soil treatments, suggesting that As(III) inhibited microbial Fe(II) oxidation and that the arsenic-oxidizing bacteria were more active than the FeOB in the As(III) treatments. Michel et al. (2007) also concluded that the specific As(III)-oxidase activity of the arsenic-oxidizing bacteria induced by As(III) is stronger than that of the FeOB. These results indicate that both the iron- and arsenic-oxidizing bacteria are responsible for As(III) oxidation although the As(III)-oxidizing bacteria may not be the main microorganisms in micro-oxic environments.

## 5. CONCUSIONS AND IMPLICATIONS

The micro-oxic conditions in the rhizosphere and at the water-soil interface of iron-rich paddy soil are widely distributed due to the repeated flooding and drying of the soils and sediments. In these areas, microaerophilic microorganisms, such as iron- and arsenic-oxidizing bacteria, can induce the formation of Fe(III) oxyhydroxide minerals with a large specific surface area. These biogenic Fe(III) oxyhydroxides co-precipitate and/or adsorb both As(III) and As (V), reducing the mobility and bioavailability of the arsenic. Therefore, it is critical to understand the microbial processes involving in the Fe(II) oxidation, mineralization, and arsenic transformation occurring in micro-oxic conditions. Our results show that efficient arsenic immobilization occurs during microaerophilic Fe(II) oxidation due to the preferential co-precipitation of arsenic with Fe(III) oxyhydroxides in comparison to sorption. Additionally, most of the arsenic in the precipitate existed as As(V) in the As (III) treatments, indicating that As(III) oxidation occurred prior to arsenic immobilization. The *aioA* gene and *aioA*/16S rRNA gene ratio results suggested the potential contributions of arsenic-oxidizing bacteria to the biotic oxidation of As(III). As(V) was preferentially adsorbed onto and co-precipitated with the Fe(III) oxyhydroxides due to the stronger affinity of As(V) for Fe(III) oxyhydroxides compared with that of As(III). Thus, microbial As(III) oxidation accelerated the attenuation of arsenic concentrations and significantly controlled the behavior of arsenic in micro-oxic conditions. The microbial communities involved in iron- and arsenic-oxidization presented a promising pollution control strategy for arsenic immobilization and for reducing arsenic uptake by plants in contaminated soils. Nevertheless, further studies should be conducted to isolate and identify FeOB in oxic-anoxic transition zones, which would be helpful in establishing and elucidating the links between Fe(II) oxidation and metal cycling.

## ACKNOWLEDGEMENTS

We thank Prof. Shaoming Li from Shandong University for making language edits and corrections. This research was supported by the National Science Foundation of China (41603127, U1612442 and U1701241), the National Key Research and Development Program of China (2017YFD0801000), the Frontier Science Research Programme of the Chinese Academy of Sciences (CAS) (QYZDB-SSW-DQC046), the Special Fund for Agro-Scientific Research in the Public Interest of China (201503107), the Science and Technology Foundation of Guangdong, China (2016A030313780, 2016TX03Z086 and 2017BT01Z176), and GDAS' Project of Science and Technology Development (2018GDASCX-0928 and 2019GDASYL-0301002).

## NOTES

The authors declare no competing financial interests.

## RESEARCH DATA

The data are included in the manuscript.

## APPENDIX A. SUPPLEMENTARY MATERIAL

X-ray photoelectron spectroscopy (XPS); Mössbauer spectroscopy; bacteria colony morphology; SEM images; bioinformatics analysis; treatment methods; Mössbauer spectral parameters; summary of sequences. Supplementary data to this article can be found online at https://doi.org/10.1016/j.gca.2019.09.002.

## REFERENCES


Bissen M. and Frimmel F. H. (2003) Arsenic-a review. Part II: oxidation of arsenic and its removal in water treatment. *Clean: Soil, Air, Water* **31**, 97–107.

Borch T., Kretzschmar R., Kappler A., Cappellen P. V., Ginder-Vogel M., Voegelin A. and Campbell K. (2009) Biogeochemical redox processes and their impact on contaminant dynamics. *Environ. Sci. Technol.* **44**, 15–23.

Cánovas D., Cases I. and De Lorenzo V. (2003) Heavy metal tolerance and metal homeostasis in *Pseudomonas putida* as revealed by complete genome analysis. *Environ. Microbiol.* **5**, 1242–1256.

Casiot C., Morin G., Juillot F., Bruneel O., Personné J. C., Leblanc M., Duquesne K., Bonnefoy V. and Elbaz-Poulichet F. (2003) Bacterial immobilization and oxidation of arsenic in acid mine drainage (Carnoulès creek, France). *Water Res.* **37**, 2929–2936.

Chan C., Emerson D. and Luther, III, G. (2016) The role of microaerophilic Fe-oxidizing microorganisms in producing banded iron formations. *Geobiology* **14**, 509–528.

Chen C., Barcellos D., Richter D. D., Schroeder P. A. and Thompson A. (2019) Redoximorphic Bt horizons of the Calhoun CZO soils exhibit depth-dependent iron-oxide crystallinity. *J. Soil Sediment* **19**, 785–797.

Chen Y., Li X., Liu T. and Li F. (2017) Microaerobic iron oxidation and carbon assimilation and associated microbial community in paddy soil. *Acta Geochim.* **36**, 502–505.

Ding W., Xu J., Chen T., Liu C., Li J. and Wu F. (2018) Co-oxidation of As (III) and Fe (II) by oxygen through complexation between As (III) and Fe(II)/Fe(III) species. *Water Res.* **143**, 599–607.

Dixit S. and Hering J. G. (2003) Comparison of arsenic(V) and arsenic(III) sorption onto iron oxide minerals: implications for arsenic mobility. *Environ. Sci. Technol.* **37**, 4182–4189.

Edwards K. J., Rogers D. R., Wirsen C. O. and McCollom T. M. (2003) Isolation and characterization of novel psychrophilic, neutrophilic Fe-oxidizing, chemolithoautotrophic α- and γ-Proteobacteria from the deep sea. *Appl. Environ. Microbiol.* **69**, 2906–2913.

Emerson D., Fleming E. J. and McBeth J. M. (2010) Iron-oxidizing bacteria: an environmental and genomic perspective. *Annu. Rev. Microbiol.* **64**, 561–583.

Emerson D. and Moyer C. (1997) Isolation and characterization of novel iron-oxidizing bacteria that grow at circumneutral pH. *Appl. Environ. Microbiol.* **63**, 4784–4792.

Emerson D., Rentz J. A., Lilburn T. G., Davis R. E., Aldrich H., Chan C. and Moyer C. L. (2007) A novel lineage of proteobacteria involved in formation of marine Fe-oxidizing microbial mat communities. *PLoS One* **2**, e667.

Fernandez-Rojo L., Héry M., Le Pape P., Braungardt C., Desoeuvre A., Torres E., Tardy V., Resongles E., Laroche E. and Delpoux S. (2017) Biological attenuation of arsenic and iron in a continuous flow bioreactor treating acid mine drainage (AMD). *Water Res.* **123**, 594–606.

Fleming E. J., Cetinić I., Chan C. S., King D. W. and Emerson D. (2014) Ecological succession among iron-oxidizing bacteria. *ISME J.* **8**, 804–815.

Fleming E. J., Langdon A. E., Martinez-Garcia M., Stepanauskas R., Poulton N. J., Masland E. D. P. and Emerson D. (2011) What's new is old: resolving the identity of *Leptothrix ochracea* using single cell genomics, pyrosequencing and FISH. *PLoS One* **6**, e17769.

Fredrickson J. K. and Gorby Y. A. (1996) Environmental processes mediated by iron-reducing bacteria. *Curr. Opin. Biotech.* **7**, 287–294.

Fuller C. C., Davis J. A. and Waychunas G. A. (1993) Surface chemistry of ferrihydrite: Part 2. Kinetics of arsenate adsorption and coprecipitation. *Geochim. Cosmochim. Acta* **57**, 2271–2282.

Hassan Z., Sultana M., Westerhoff H. V., Khan S. I. and Röling W. F. (2016) Iron cycling potentials of arsenic contaminated groundwater in Bangladesh as revealed by enrichment cultivation. *Geomicrobiol. J.* **33**, 779–792.

Heller M. I., Lam P. J., Moffett J. W., Till C. P., Lee J. M., Toner B. M. and Marcus M. A. (2017) Accumulation of Fe oxyhydroxides in the Peruvian oxygen deficient zone implies non-oxygen dependent Fe oxidation. *Geochim. Cosmochim. Acta* **211**, 174–193.

Henke K. (2009) *Arsenic: Environmental Chemistry, Health Threats and Waste Treatment*. John Wiley & Sons, London.

Hohmann C., Winkler E., Morin G. and Kappler A. (2009) Anaerobic Fe(II)-oxidizing bacteria show As resistance and immobilize As during Fe(III) mineral precipitation. *Environ. Sci. Technol.* **44**, 94–101.

Huhmann B. L., Neumann A., Boyanov M. I., Kemner K. M. and Scherer M. M. (2017) Emerging investigator series: As(V) in magnetite: incorporation and redistribution. *Environ. Sci. Proc. Imp.* **19**, 1208–1219.

Jia Y. and Demopoulos G. P. (2005) Adsorption of arsenate onto ferrihydrite from aqueous solution: influence of media (sulfate vs nitrate), added gypsum, and pH alteration. *Environ. Sci. Technol.* **39**, 9523–9527.

Jia Y., Huang H., Chen Z. and Zhu Y. G. (2014) Arsenic uptake by rice is influenced by microbe-mediated arsenic redox changes in the rhizosphere. *Environ. Sci. Technol.* **48**, 1001–1007.

Kato S., Chan C., Itoh T. and Ohkuma M. (2013) Functional gene analysis of freshwater iron-rich flocs at circumneutral pH and isolation of a stalk-forming microaerophilic iron-oxidizing bacterium. *Appl. Environ. Microbiol.* **79**, 5283–5290.

Kumarathilaka P., Seneweera S., Meharg A. and Bundschuh J. (2018) Arsenic speciation dynamics in paddy rice soil-water environment: sources, physico-chemical, and biological factors-a review. *Water Res.* **140**, 403–414.

Lin C., Larsen E. I., Nothdurft L. D. and Smith J. (2012) Neutrophilic, microaerophilic Fe(II)-oxidizing bacteria are ubiquitous in aquatic habitats of a subtropical Australian coastal catchment (ubiquitous feob in catchment aquatic habitats). *Geomicrobiol. J.* **29**, 76–87.

Liu Z., Lozupone C., Hamady M., Bushman F. and Knight R. (2007) Short pyrosequencing reads suffice for accurate microbial community analysis. *Nucleic Acids Res.* **35**, e120.

Lieutaud A., Lis R., Duval S., Capowiez L., Muller D., Lebrun R., Lignon A., Fardeau M., Lett M., Nitschke W. and Schoepp-Cothenet B. (2010) Arsenite oxidase from *Ralstonia* sp. 22

Characterization of the enzyme and its interaction with soluble cytochromes. *J. Biol. Chem.* **285**, 20433–20441.
Meharg A. A. and Rahman M. M. (2003) Arsenic contamination of Bangladesh paddy field soils: implications for rice contribution to arsenic consumption. *Environ. Sci. Technol.* **37**, 229–234.
Meharg A. A. and Zhao F.-J. (2012) *Arsenic & Rice*. Springer Science & Business Media.
Melton E. D., Swanner E. D., Behrens S., Schmidt C. and Kappler A. (2014) The interplay of microbially mediated and abiotic reactions in the biogeochemical Fe cycle. *Nat. Rev. Microbiol.* **12**, 797.
Michel C., Jean M., Coulon S., Dictor M. C., Delorme F., Morin D. and Garrido F. (2007) Biofilms of As(III)-oxidising bacteria: formation and activity studies for bioremediation process development. *Appl. Microbiol. Biot.* **77**, 457–467.
Mitsunobu S., Hamanura N., Kataoka T. and Shiraishi F. (2013) Arsenic attenuation in geothermal streamwater coupled with biogenic arsenic(III) oxidation. *Appl. Geochem.* **35**, 154–160.
Muehe E. M. and Kappler A. (2014) Arsenic mobility and toxicity in South and South-east Asia-a review on biogeochemistry, health and socio-economic effects, remediation and risk predictions. *Environ. Chem.* **11**, 483–495.
Nitzsche K. S., Weigold P., Lösekann-Behrens T., Kappler A. and Behrens S. (2015) Microbial community composition of a household sand filter used for arsenic, iron, and manganese removal from groundwater in Vietnam. *Chemosphere* **138**, 47–59.
Picardal F. W., Zaybak Z., Chakraborty A., Schieber J. and Szewzyk U. (2011) Microaerophilic, Fe(II)-dependent growth and Fe(II) oxidation by a *Dechlorospirillum* species. *FEMS Microbiol. Lett.* **319**, 51–57.
Quéméneur M., Cébron A., Billard P., Battaglia-Brunet F., Garrido F., Leyval C. and Joulian C. (2010) Population structure and abundance of arsenite-oxidizing bacteria along an arsenic pollution gradient in waters of the Upper Isle River Basin, France. *Appl. Environ. Microbiol.* **76**, 4566–4570.
Ratering S. and Schnell S. (2001) Nitrate-dependent iron (II) oxidation in paddy soil. *Environ. Microbiol.* **3**, 100–109.
Schädler S., Burkhardt C., Hegler F., Straub K., Miot J., Benzerara K. and Kappler A. (2009) Formation of cell-iron-mineral aggregates by phototrophic and nitrate-reducing anaerobic Fe(II)-oxidizing bacteria. *Geomicrobiol. J.* **26**, 93–103.
Senn A. C., Kaegi R., Hug S. J., Hering J. G., Mangold S. and Voegelin A. (2015) Composition and structure of Fe(III)-precipitates formed by Fe(II) oxidation in water at near-neutral pH: Interdependent effects of phosphate, silicate and Ca. *Geochim. Cosmochim. Acta* **162**, 220–246.
Shelobolina E., Konishi H., Xu H., Benzine J., Xiong M. Y., Wu T., Blöthe M. and Roden E. (2012) Isolation of phyllosilicate-iron redox cycling microorganisms from an illite-smectite rich hydromorphic soil. *Front. Microbiol.* **3**, 134.
Slyemi D. and Bonnefoy V. (2012) How prokaryotes deal with arsenic. *Environ. Microbiol. Rep.* **4**, 571–586.
Smedley P. and Kinniburgh D. (2002) A review of the source, behaviour and distribution of arsenic in natural waters. *Appl. Geochem.* **17**, 517–568.
Smith R. L., Kent D. B., Repert D. A. and Böhlke J. K. (2017) Anoxic nitrate reduction coupled with iron oxidation and attenuation of dissolved arsenic and phosphate in a sand and gravel aquifer. *Geochim. Cosmochim. Acta* **196**, 102–120.
Sowers T. D., Harrington J. M., Polizzotto M. L. and Duckworth O. W. (2017) Sorption of arsenic to biogenic iron(oxyhydr) oxides produced in circumneutral environments. *Geochim. Cosmochim. Acta* **198**, 194–207.
Sø H. U., Postma D., Hoang V. H., Mai L. V., Kim T. P., Hung V. P. and Jakobsen R. (2018) Arsenite adsorption controlled by the iron oxide content of Holocene Red River aquifer sediment. *Geochim. Cosmochim. Acta* **239**, 61–73.
Sun W., Sierra-Alvarez R., Milner L., Oremland R. and Field J. A. (2009) Arsenite and ferrous iron oxidation linked to chemolithotrophic denitrification for the immobilization of arsenic in anoxic environments. *Environ. Sci. Technol.* **43**, 6585–6591.
Swanner E. D., Nell R. M. and Templeton A. S. (2011) *Ralstonia* species mediate Fe-oxidation in circumneutral, metal-rich subsurface fluids of Henderson mine, CO. *Chem. Geol.* **284**, 339–350.
Swanner E. D., Wu W., Schoenberg R., Byrne J., Michel F. M., Pan Y. and Kappler A. (2015) Fractionation of Fe isotopes during Fe(II) oxidation by a marine photoferrotroph is controlled by the formation of organic Fe-complexes and colloidal Fe fractions. *Geochim. Cosmochim. Acta* **165**, 44–61.
Tao L., Zhang W., Li H., Li F., Yu W. and Chen M. (2012) Effect of pH and weathering indices on the reductive transformation of 2-nitrophenol in south China. *Soil Sci. Soc. Am. J.* **76**, 1579–1591.
Tian Z., Feng Y., Guan Y., Shao B., Zhang Y. and Wu D. (2017) Opposite effects of dissolved oxygen on the removal of As(III) and As(V) by carbonate structural Fe(II). *Sci. Rep.* **7**, 17015.
Tong H., Hu M., Li F., Liu C. and Chen M. (2014) Biochar enhances the microbial and chemical transformation of pentachlorophenol in paddy soil. *Soil Biol. Biochem.* **70**, 142–150.
Voegelin A., Kaegi R., Frommer J., Vantelon D. and Hug S. J. (2010) Effect of phosphate, silicate, and Ca on Fe(III)-precipitates formed in aerated Fe(II)- and As(III)-containing water studied by X-ray absorption spectroscopy. *Geochim. Cosmochim. Acta* **74**, 164–186.
Von Rozycki T. and Nies D. H. (2009) *Cupriavidus metallidurans*: evolution of a metal-resistant bacterium. *Anton. Leeuw.* **96**, 115–139.
Weber K. A., Achenbach L. A. and Coates J. D. (2006) Microorganisms pumping iron: anaerobic microbial iron oxidation and reduction. *Nat. Rev. Microbiol.* **4**, 752.
Weiss J. V., Emerson D. and Megonigal J. P. (2004) Geochemical control of microbial Fe(III) reduction potential in wetlands: comparison of the rhizosphere to non-rhizosphere soil. *FEMS Microbiol. Ecol.* **48**, 89–100.
Weiss J. V., Rentz J. A., Plaia T., Neubauer S. C., Merrill-Floyd M., Lilburn T., Bradburne C., Megonigal J. P. and Emerson D. (2007) Characterization of neutrophilic Fe(II)-oxidizing bacteria isolated from the rhizosphere of wetland plants and description of *Ferritrophicum radicicola* gen. nov. sp. nov., and *Sideroxydans paludicola* sp. nov. *Geomicrobiol. J.* **24**, 559–570.
Whelan J. A., Russell N. B. and Whelan M. A. (2003) A method for the absolute quantification of cDNA using real-time PCR. *J. Immunol. Methods* **278**, 261–269.
Wu Y., Kukkadapu R. K., Livi K. J., Xu W., Li W. and Sparks D. L. (2018) Iron and arsenic speciation during As(III) oxidation by manganese oxides in the presence of Fe(II): molecular-level characterization using XAFS, Mössbauer, and TEM analysis. *ACS Earth Space Chem.* **2**, 256–268.
Xiu W., Guo H., Liu Q., Liu Z. and Zhang B. (2015) Arsenic removal and transformation by *Pseudomonas* sp. strain GE-1-induced ferrihydrite: co-precipitation versus adsorption. *Water Air Soil Poll.* **226**, 167.
Xiu W., Guo H., Shen J., Liu S., Ding S., Hou W., Ma J. and Dong H. (2016) Stimulation of Fe(II) oxidation, biogenic lepi-

docrocite formation, and arsenic immobilization by *Pseudogulbenkiania* sp. strain 2002. *Environ. Sci. Technol.* **50**, 6449–6458.
Zhang S. Y., Zhao F. J., Sun G. X., Su J. Q., Yang X. R., Li H. and Zhu Y. G. (2015) Diversity and abundance of arsenic biotransformation genes in paddy soils from southern China. *Environ. Sci. Technol.* **49**, 4138–4146.
Zhang X., Wu M., Dong H., Li H. and Pan B. C. (2017) Simultaneous oxidation and sequestration of As(III) from water by using redox polymer-based Fe(III) oxide nanocomposite. *Environ. Sci. Technol.* **51**, 6326–6334.

*Associate editor:* Hailiang Dong